29 Mar 2001, 4:00 pm - 6:00 pm

Measurement of G_{max} and K_0 of Saturated Clay Using Bender Elements

Bartlomiej Grolewski
University of Kentucky, Lexington, KY

Xiangwu Zeng
Case Western Reserve University, Cleveland, OH

MEASUREMENT OF G_{MAX} AND K_0 OF SATURATED CLAY USING BENDER ELEMENTS

Bartlomiej Grolewski
University of Kentucky
Lexington, KY 40506

Xiangwu Zeng
Case Western Reserve University
Cleveland, OH 44106-7201

ABSTRACT

Recent development in the application of bender element technique has made it possible to measure G_{max} and K_0 of soils under complex anisotropic loading conditions. By measuring the shear wave velocities in different shear planes, the anisotropy in G_{max} of soil induced by anisotropic loading can be determined. The shear wave velocities can also be used to calculate the horizontal earth pressure coefficient at rest K_0.

This paper reports an experimental setup developed at the Department of Civil Engineering, University of Kentucky, which uses bender elements to measure shear wave velocities in four shear planes in a saturated clay specimen under different consolidation pressure. The data is used to investigate the anisotropy of soil stiffness in clay due to anisotropic stress conditions. The measured G_{max} is compared with the calculation by several empirical formulae. The measured G_{max} on different shear planes are also used to calculate K_0 of clay under different consolidation pressure and compared with results of empirical theories. The applied stress condition includes loading, unloading, and reloading of up to 22 cycles, thus allowed us to study the influence of repeated loading on G_{max} and K_0 of clay. The study is funded by the National Science Foundation.

INTRODUCTION

Anisotropy of materials is often overlooked in studies of parameters defining material behavior. Such a simplification of the problem can introduce significant errors leading to incorrect engineering solutions. In fact, virtually all soil materials in their natural state exhibit some anisotropy. This anisotropy can be due to the fabric of the soil or state of existing stresses.

Shear modulus is an important soil parameter that describes material behavior under shear stresses. Shear modulus, however, changes with shear strain. The highest value of shear modulus is called initial shear modulus (G_0), or maximum shear modulus (G_{max}). Maximum shear modulus has great importance in earthquake engineering, since most damage caused to ground structures comes from earthquake shear forces. These seismic forces in most cases induce very small strains in soil layers they go through and, therefore, the use of G_{max} is appropriate to represent dynamic properties of soils. G_{max} can be used in problems related to foundation vibrations, seismic slope stability, impact of earthquake waves upon surface structures, etc.

There are some previous research focused on an accurate measurement of elastic shear modulus of soils. Hardin and Drnevich (1972) used three devices to measure G_{max} at strain level of 0.025% and established parameter influence on the modulus. Roesler (1979) proved that shear wave velocity depends on the direction of propagation and polarization, but not the orthogonal direction. Lanzo et al (1997), with the use of simple shear device, studied the influence of the overconsolidation ration and plasticity index upon normalized shear modulus reduction curves. Hryciw (1990) created a model for calculating G_{max} by using data from dilatometer testing, and Kita (1992) showed high dependency of G_{max}

upon confining pressure using centrifuge testing. In 1985, Dyvik and Madhaus published bender elements procedure of testing. Their research was followed by Zeng and Ni (1998a) who tested dry sand under K_0 loading in oedometer with bender elements. Joivicic and Coop (1998) installed benders in triaxial apparatus and measured G_{max} of London clay and kaolin samples.

An existing theory regarding elastic shear modulus can help verifying the experimental results. In 1989, Hardin and Blandford published an elastic constitutive equation, which defines G_{max} in planes containing principal stresses:

$$G_{\max} = \frac{OCR^k}{F(e)} \frac{S_{ij}}{2(1+\upsilon)} p_a^{1-n} (\sigma'_i \sigma'_j)^{n/2} \quad \text{.....(1)}$$

where: σ'_i, σ'_j = effective stresses in the plane G_{max} is to be found; OCR = overconsolidation ratio; k = constant dependant on plasticity index PI; n = elastic constant; ν = Poisson' s ratio; S_{ij} = dimensionless elastic stiffness constant; p_a = atmospheric pressure; F(e) = function of void ratio = $0.3 + 0.7e^2$.

Equation 1 is applicable for finding elastic modulus in the plane of principal stresses. For any plane non-coincidental with the principal stresses, Zeng and Ni (1998b) suggested that G_α should equal to:

$$G_\alpha = \frac{G_V G_H}{G_H \sin^2 \alpha + G_V \cos^2 \alpha} \quad \text{.....(2)}$$

where α is an inclination angle of G_α plane with respect to horizontal plane.

EXPERIMENTAL SETUP

Soil index properties tests were carried out to establish basic properties of the Lexington Clay to be tested with bender elements. Atterberg limits revealed the liquid limit to be 50 and plastic limit of 22. The specific gravity of Lexington Clay was determined to be 2.71. One-dimensional consolidation testing produced the following results: coefficient of consolidation (C_v) of $3.5 \cdot 10^{-4}$ cm^2/s, coefficient of compressibility (C_c) of 0.416, and coefficient of rebound (C_r) of 0.048 for slurry samples.

Bender elements were chosen as a means of measuring the elastic shear modulus, because the energy they introduce into a sample is very small, thus producing insignificant strains. To test the Lexington Clay samples, bender elements were mounted in an oedometer apparatus. The driving signal was supplied by Wavetek Pulse Generator, and the receiving signal was displayed on HP Digitizing Oscilloscope. Then, the data was collected by PC Data Acquisition system (see Figure 1 below). The oedometer itself was placed in a 1-D consolidation machine, which applied load to the tested sample by a means of house pressure.

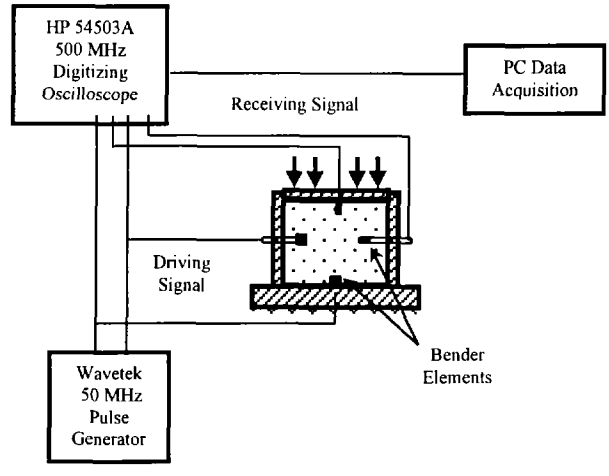

Figure 1: Electrical Setup

The load was vertically transmitted to the sample with the use of oedometer cap. The oedometer rigidity is adequate to provide K_0 loading. Two pairs of benders were mounted in the oedometer, horizontal transmitter and receiver, and vertical transmitter and receiver (see Figure 2).

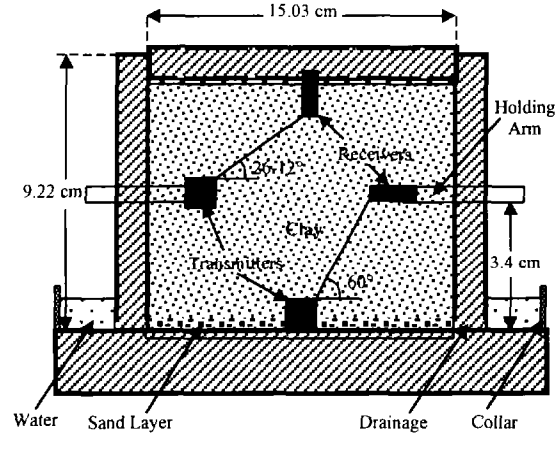

Figure 2: Oedometer Detailed Schematic

Vertical benders were mounted directly into the cap and the base of the oedometer. Horizontal benders were placed into holding arms. By adjusting the location of the holding arms, the horizontal benders could be properly positioned with respect to vertical ones in order to achieve 60 and 30 (and less) degree angles for horizontal transmitter to vertical receiver, and vertical transmitter to horizontal receiver

directions, respectively. Small holes were drilled near the bottom of the oedometer wall and in the cap to allow for excess pore pressure dissipation. Then, water holding rubber collar was attached to the sides of the oedometer base to keep the sample saturated.

Two samples of Lexington clay were tested. The moisture contents of samples were 43.6 and 45.4 percent. The initial void ratios were 1.31 and 1.35. The samples were assumed to be fully saturated. The loading was applied in 50 kPa increments up to 300 kPa, which was chosen by considering the limitations of the consolidation apparatus and the house pressure. Since the tested samples were cohesive soils and no pore pressure measurement was devised, adequate time had to be allowed for pore pressure dissipation before taking readings and increasing the loading.

EXPERIMENTAL RESULTS AND INTERPRETATION

Bender Elements Testing

Shear wave generated and received by benders covers the distance between the elements in a certain time. By measuring this time, shear wave velocity can be determined:

$$v_s = \frac{d}{t} \quad \text{.....(3)}$$

where d is the distance between the elements (tip to tip), and t the arrival time.

Elastic shear modulus is related to the velocity with soil density (ρ) by:

$$G_{max} = \rho \cdot v^2 \quad \text{.....(4)}$$

The shear wave arrival time was obtained from oscilloscope readings. The first wave arrival is characterized by sudden rise in the wave pattern (voltage). The scope was setup so the trigger time occurred at point zero. Thus by reading off the arrival time, the travel time was known instantly. The arrival point was taken as the first initial rise in the pattern, not the first peak.

The behavior of Lexington clay sample under K_0 loading is presented in Figures 3-7. The first figure of that series (Figure 3) shows G_{max} distribution in all four directions during the first loading. The values of elastic shear modulus form curves, which are slightly concave down. Depending on direction of shear wave propagation, the curves (trends) are shifted with respect to one another. The lowest curve (lowest G_{max} values) represents the shear modulus in the horizontal shear plane (G_h). Above the horizontal, the horizontal-vertical direction (26.2-12.7 degree angles) curve lays, which represents G_{hv} followed by the vertical-horizontal (60 degree angle) plane (G_{vh}) and vertical plane (G_v). At the lowest pressure point, the data points are scattered close to each other, while at the highest pressure point the scatter is bigger.

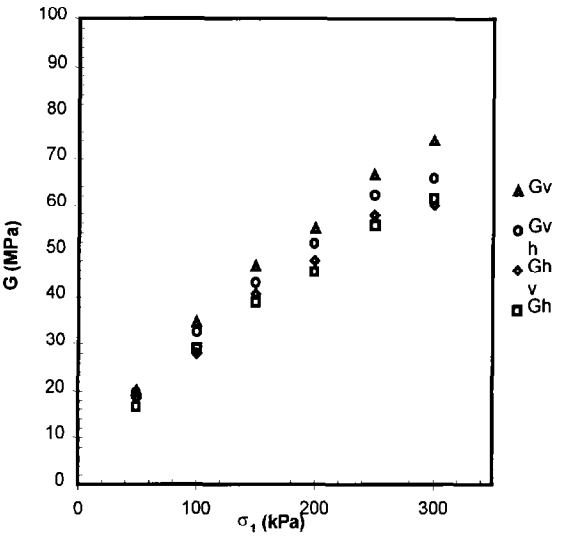

Figure 3: G_{max} in Four Directions vs. Vertical Pressure Graph for First Loading

The following four figures (Figures 4-7) show the behavior of the sample during all 22 cycles of loading. The first unloading curves do not follow the loading ones. They are shifted upwards and pivoted about the highest pressure points. This strengthening comes from the past loading history and overconsolidation ratio. As the sample is unloaded, it " feels" the past highest overburden stress, which made the sample denser and stronger. The second loading cycle is characterized by a much smaller shift and rotation. Here, the shift resembles a hysteric shape (a loop) which is a proof of energy dissipation during the complete cycle. After the first two full cycles, eight partial ones were applied (50 and 300 kPa pressure points). These partial cycles introduce further sample strengthening, however, the effect is more pronounced for the first partial cycles and less for the last ones. The 11th and 12th cycles are the full ones. They produce similar hysteretic loops such as the second full cycle. These loops seem to introduce less energy dissipation since the areas bound by them are smaller. The next 8 partial cycles do not have much influence on the sample behavior. The curves are minimally shifted, and the last two full cycles almost plot on the top of each other.

Comparison with Hardin-Blandford Theory

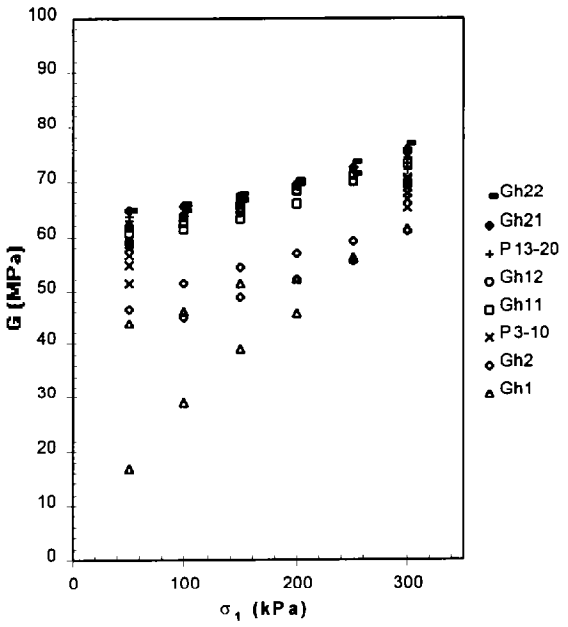

Figure 4: G_h Distribution for Lexington Clay for 22 Cycles

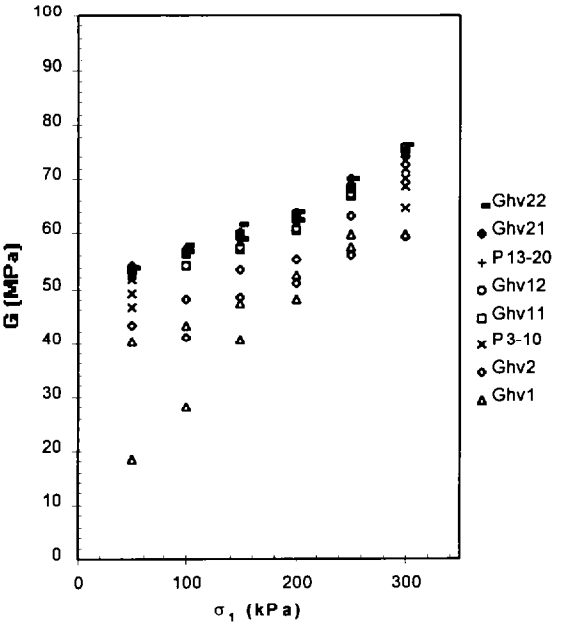

Figure 6: G_{hv} Distribution for Lexington Clay for 22 Cycles

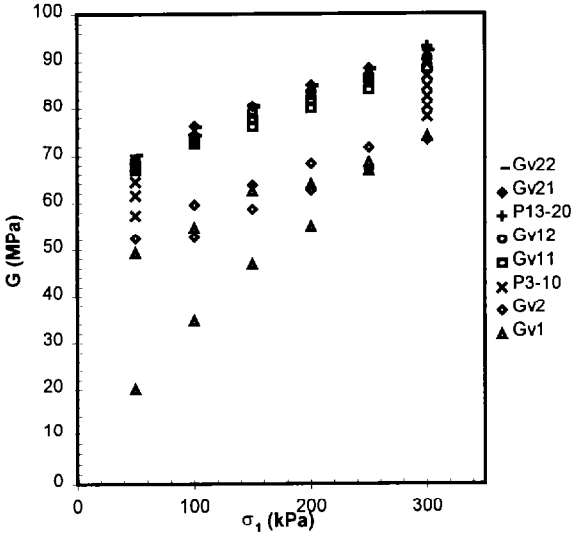

Figure 5: G_v Distribution for Lexington Clay for 22 Cycles

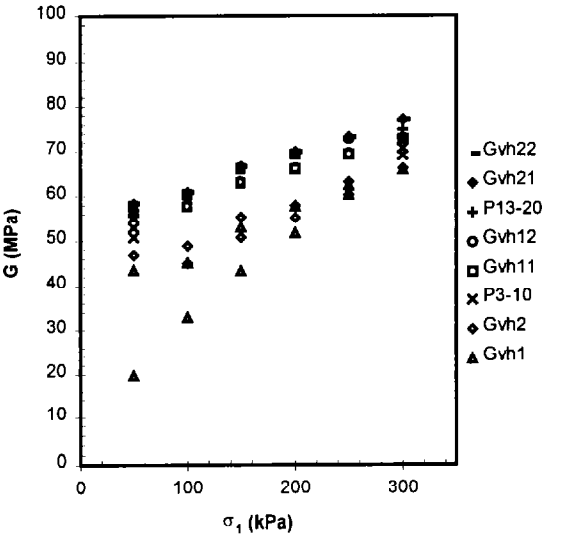

Figure 7: G_{vh} Distribution for Lexington Clay for 22 Cycles

Legend:
Gv- vertical transmitter to vertical receiver
Gvh- vertical transmitter to horizontal receiver
Ghv- horizontal transmitter to vertical receiver
Gh- horizontal transmitter to horizontal receiver

Gh1- 1st full cycle
P3-9- 3rd through 9th partial cycle
P13-20- 13th through 20th partial cycle

The first verification of results comes from checking the experimental data points against the predicted ones based on Hardin-Blandford constitutive equation (Eq. 1). Figure 8 and 9 show first loading cycle and include both experimental and empirical data points in horizontal and vertical directions.

An agreement of experimental points with theoretical ones is very good. Hardin-Blandford equation accurately predicts both loading and unloading patterns. The unloading upward shift is taken into consideration with inclusion of overconsolidation ratio raised to a power k based on the soil plasticity index (PI). The value of k is 0.23.

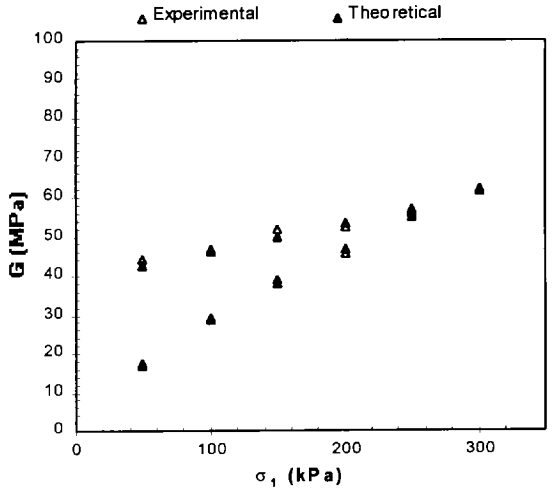

Figure 8: Experimental and Theoretical G_h of Lexington Clay

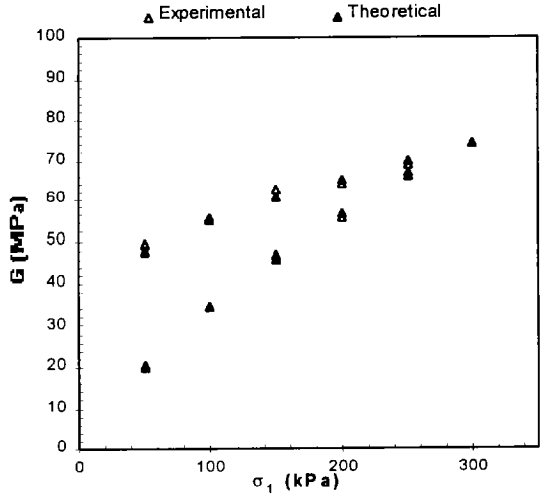

Figure 9: Experimental and Theoretical G_v of Lexington Clay

Estimation of S_{ij}.

The elastic stiffness coefficient (S_{ij}) appearing in the Hardin-Blandford constitutive equation does not depend on a single state of soil. For different states of stresses, S_{ij} will stay constant. Because of this behavior, the stiffness coefficient is related to soil reference fabric. It also expresses the anisotropy of the sample.

To obtain a value of the elastic stiffness coefficient, values of G_{max} were calculated and then divided by the right side of Equation 1 so that the ratio of $[S_{ij}/2(1+\nu)]$ could be determined. Figure 10 below shows the quotient distribution with respect to vertical principal stress. The values of the quotient remain constant for the first two cycles (mean value 467). Then, they increase as several partial cycles are applied (mean value 585). This phenomenon can be attributed to changes, which occur in the clay sample as it experiences more and more repetitive loading causing the sample to become stiffer. The increased density and stiffness of the sample have some effect upon the reference fabric and the elastic stiffness coefficient. Finally, after last series of partial cycles, the values of Sij increase only slightly giving a mean value of 588.

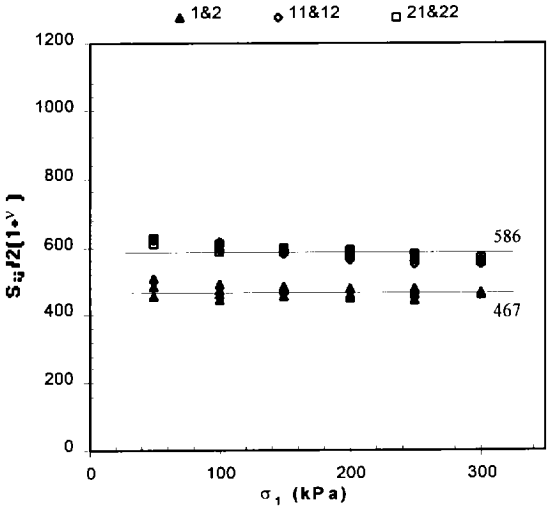

Figure 10: Evaluation of Effect of Stress History on S_{ij}

Estimation of K_0.

Accurate K_0 estimation is essential for this research, since the experimental setup did not allow for the measurement of the horizontal stresses. The principal stresses in the experiment are related to each other with K_0:

$$K_0 = \frac{\sigma_3'}{\sigma_1'} \quad \text{.....(5)}$$

The value of K_0 can also be found from shear wave velocities as reported by Zeng and Ni (1998b):

$$K_0 = \left(\frac{V_{23}}{V_{13}}\right)^{4/n} \quad \text{.....(6)}$$

where V_{23} and V_{13} are shear wave velocities in horizontal and vertical plane, respectively.

The experimental values of K_0 can be compared to empirical equations. In the case of loading, Jaky (1949) proposes that:

$$K_0 = 1 - \sin\phi' \quad \text{.....(7)}$$

where ϕ' is a soil internal friction angle.

For unloading, Mayne and Kulhawy (1982) developed the following relationship:

$$K_0 = (1 - \sin\phi')OCR^{\sin\phi'} \quad \text{.....(8)}$$

Figures 11 and 12 show experimental values of K_0 . During loading cycles, K_0 remained approximately constant, and Jacky' s equation with friction angle of 31 degrees accurately fits into the data points. For unloading, however, the Kulhawy equation has to be modified to fit the data. The following equation introduces parameters a and b and better fits into the data points:

$$K_0 = a(1 - \sin\phi')OCR^{b\sin\phi} \quad \text{.....(9)}$$

In the case of Lexington Clay, the values for a and b are 0.90 and 0.45, respectively.

Shear Modulus in Different Planes.

Shear modulus values in sloping planes (other than vertical and horizontal) can be predicted by Zeng-Ni equation. According to their theory, G_α, where $0<\alpha<90$, is smaller than the G_v and larger than G_h. The values of G_α should follow an ellipse with semiaxis equal to $G_v^{0.5}$ and $G_h^{0.5}$. Figure 13 presents both experimental values of G_α and theoretical values based on Zeng-Ni equation for Lexington clay. The experimental points fall reasonably well along the paths defined by the equation. This is true for both G_{vh} which lies on plane sloped 60 degree with respect to horizontal plane, and G_{hv} which changed slope as more pressure was applied ($26.2^\circ<\alpha<12.7^\circ$).

Influence of Cyclic Loading.

The influence of cyclic loading was investigated by applying several full and partial loading cycles to Lexington clay. Strengthening effect is visible as the sample is repeatedly compacted in the 1-D consolidation apparatus (see Figure 14). This effect is most visible during the first series of cycles. The hysteretic shape is mostly pronounced for the first cycle. The energy loss during this cycle is the greatest. Then it decreases as the sample experiences the effects of past pressure history. Next, eight partial cycles move the curves up a considerable amount. The following two full cycles exhibit much smaller dissipation energy and " skinnier" hysteretic shape. The last eight partial cycles bring little more strengthening. The last two full cycles plot very close to each other.

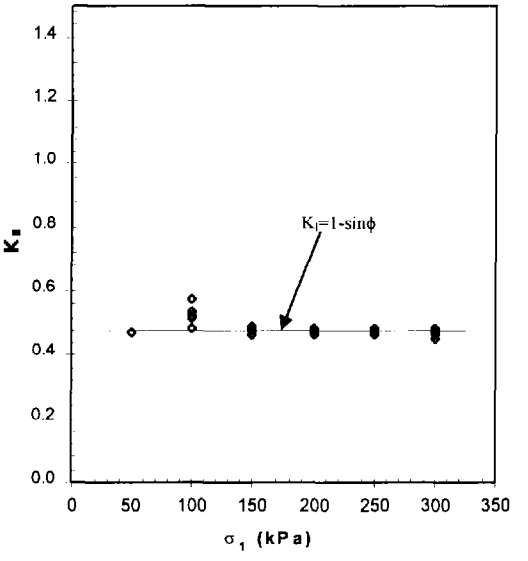

Figure 11: Empirical and Experimental K_0 Comparison-Loading

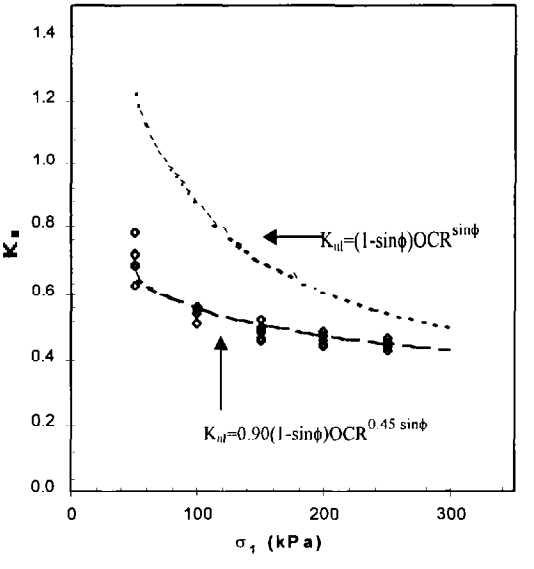

Figure 12: Empirical and Experimental K_0 Comparison-Unloading

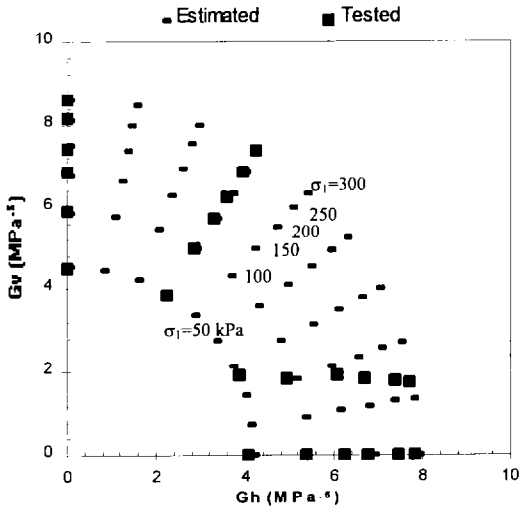

Figure 13: Shear Modulus in Different Planes

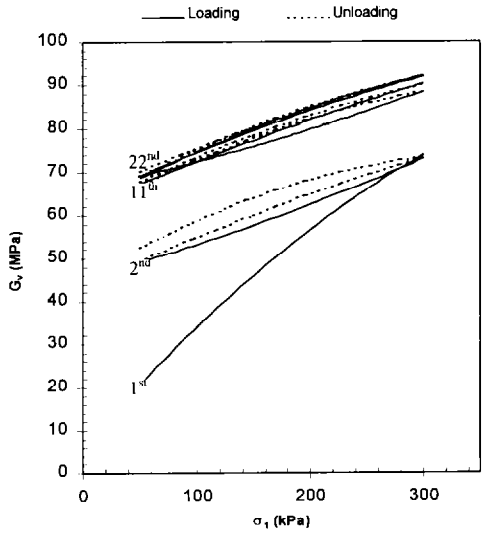

Figure 14: Influence of Cyclic Loading upon G_v

CONCLUSIONS

Measurements of arrival times of shear waves with the use of bender elements turn out to be a very effective way of determining the effect of anisotropic loading upon elastic shear modulus of cohesive soils. Shear wave velocities and elastic shear moduli can be easily calculated from travel times and distances. With the use of benders, determination of G_{max} behavior on different planes of soil specimen under anisotropic loading (K_0 loading) produced meaningful results. The patterns obtained for elastic shear modulus both in horizontal and vertical planes compare well with empirical constitutive equation derived by Hardin and Blandford. The results of G_{max} in other directions agree with Zeng-Ni equation.

The effect of cyclic loading was investigated up to 22 cycles. There was observed a shear stiffness increase in the sample as the cycles progressed, and the rate of increase decrease with the number of cycles.

ACKNOWLEDGMENT

The study reported here was supported by the grant CMS 9728860 from the National Science Foundation. The authors thank the program officer, Dr. Astill, of NSF for his support.

REFERENCES

Drnevich, V.P., Hardin, B.O., and Shippy, D.J. [1977]. " Modulus and Damping of the Soils by the Resonant Column Method" , Dynamic Geotechnical Testing, ASTM STP 654, 91-125.

Dyvik, R. and Madshus, C. [1985]. " Lab Measurements of Gmax Using Bender Elements" , Conference Proceeding, Part of: Advances in the Art of Testing Soils under Cyclic Conditions, Vijay Khosla, ed., 1985, Detroit, MI, Geotechnical Engineering Division, ASCE, New York, 186-196.

Hardin, B. O., and Black, W. L. [1969]. " Closure to Vibration Modulus of Normally Consolidated Clay" , J. Soil Mech. And Found. Div., ASCE, 95(6), 1531-1537.

Hardin, B.O. and Blandford, G. E. [1989]. " Elasticity of Particulate Materials" , Journal of Geotechnical Engineering, ASCE, 115(6), 788-805.

Hardin, B.O. and Drnevich, V.P. [1972]. " Shear Modulus and Damping in Soils: Measurement and Parameter Effects" , Journal of the Soil Mechanics and Foundation Division, ASCE, 98(6), pp. 603-624.

Hryciw, R. D. [1990]. " Small-Strain-Shear Modulus of Soil by Dilatometer" , Journal of Geotechnical Engineering, Vol. 116, No. 11, pp. 1700-1716.

Jaky, J. [1949]. " Pressure in Soils" , Proceeding of 2nd International Conference on Soil Mechanics and Foundation Engineering, 1(1), 103-107.

Jovicic, V. and Coop, M. R. [1998]. " The Measurement of Stiffness of Clays with Bender Element Tests in the Triaxial Apparatus" , Geotechnical Testing Journal, ASTM, 21(1),3-10.

Kita, K., Shibata, T., Yashima, A., and Kobayashi, S. [1992]. " Measurement of Shear Wave Velocities of Sand in a Centrifuge" , Soils and Foundations, Vol. 32, No. 2, 134-140.

Lanzo, G. [1997]." Reduction of Shear Modulus at Small Strains in Simple Shear" , Journal of Geotechnical and Geoenvironmental Engineering, Vol. 123, No. 11, 1035-1042.

Mayne, P. W. and Kulhawy, F. W. [1982]. " K_0-OCR Relationships in Soils" , Journal of Geotechnical Engineering, ASCE, 108(6), 851-872.

Roesler, S. K. [1979]. " Anisotropic Shear Modulus due to Stress Anisotropy" , Journal of Geotechnical Engineering, ASCE, 105(7), 871-880.

Zeng, X., and Ni, B. [1998a]. " Application of Bender Elements in Measuring G_{max} of Sand under K_0 Condition" , Geotechnical Testing Journal, Vol. 21, No. 3, 251-263.

Zeng, X., and Ni, B. [1998b]. " Measurement of G_{max} of Sand under Anisotropic Loading Condition Using Bender Elements" , Geotechnical Specialty Publication No. 75, ASCE, 189-200.